

UC Irvine

UC Irvine Previously Published Works

Title

Reconstruction of Paleofire Emissions Over the Past Millennium From Measurements of Ice Core Acetylene

Permalink

<https://escholarship.org/uc/item/3m42490x>

Journal

Geophysical Research Letters, 47(3)

ISSN

0094-8276

Authors

Nicewonger, Melinda R
Aydin, Murat
Prather, Michael J
et al.

Publication Date

2020-02-16

DOI

10.1029/2019gl085101

Peer reviewed

Geophysical Research Letters

RESEARCH LETTER

10.1029/2019GL085101

Key Points:

- First ever ice core record of acetylene covering the last 2,000 years is used to reconstruct paleofire emissions
- Preindustrial acetylene levels over Antarctica were nearly double the modern-day mean level
- Inferred biomass burning emissions of acetylene from 1000 to 1500 CE are several times greater than modern-day rates and decline sharply around 1650 CE

Supporting Information:

- Supporting Information S1

Correspondence to:

M. R. Nicewonger,
nicewonm@uci.edu

Citation:

Nicewonger, M. R., Aydin, M., Prather, M. J., & Saltzman, E. S. (2020). Reconstruction of paleofire emissions over the past millennium from measurements of ice core acetylene. *Geophysical Research Letters*, 47, e2019GL085101. <https://doi.org/10.1029/2019GL085101>

Received 22 AUG 2019

Accepted 4 JAN 2020

Reconstruction of Paleofire Emissions Over the Past Millennium From Measurements of Ice Core Acetylene

Melinda R. Nicewonger¹, Murat Aydin¹, Michael J. Prather¹, and Eric S. Saltzman^{1,2}

¹Department of Earth System Science, University of California, Irvine, CA, USA, ²Department of Chemistry, University of California, Irvine, CA, USA

Abstract Acetylene is a short-lived trace gas produced during combustion of fossil fuels, biomass, and biofuels. Biomass burning is likely the only major source of acetylene in the preindustrial atmosphere, making ice core acetylene a powerful tool for reconstructing paleofire emissions. Here we present a 2,000-year atmospheric record of acetylene reconstructed from analysis of air bubbles trapped in Greenland and Antarctic ice cores and infer pyrogenic acetylene emissions using a chemistry transport model. From 0 to 1500 CE, Antarctic acetylene averages $36 \pm 1 \text{ pmol mol}^{-1}$ (mean $\pm 1 \text{ SE}$), roughly double the annual mean over Antarctica today. Antarctic acetylene declines during the Little Ice Age by over 50% to $17 \pm 2 \text{ pmol mol}^{-1}$ from 1650 to 1750 CE. Acetylene over Greenland declines less dramatically over the same period. Modeling results suggest that pyrogenic acetylene emissions during 1000–1500 CE were sustained at rates significantly greater than modern day and declined by over 50% during the 1650–1750 CE period.

Plain Language Summary Acetylene is an atmospheric trace gas produced by combustion of fossil fuels, agricultural and domestic burning, and wildfires. In the preindustrial atmosphere, the major source of acetylene is from wildfires. We measured the abundance of acetylene in the air bubbles trapped inside polar ice cores from Greenland and Antarctica over the last 2,000 years for the first time. Variations in the atmospheric abundance of acetylene over Antarctica indicate large changes in preindustrial wildfire emissions. Using a model, we find that preindustrial wildfire emissions of acetylene during the Medieval Period (1000–1500 CE) could have been several fold greater than what is observed today. Acetylene emissions declined by about 50% at the onset of the Little Ice Age (1650–1750 CE).

1. Introduction

Biomass burning (BB) impacts climate through emissions of greenhouse gases, aerosols, reactive trace gases, and by modifying surface albedo. There is debate about how BB emissions varied in the past and whether climate or human activities were the major driver of those variations (Bowman et al., 2009; Ferretti et al., 2005; Marlon et al., 2009; Mischler et al., 2009; Power et al., 2012; Sapart et al., 2012; van der Werf et al., 2013; Wang et al., 2010). There has been extensive work on reconstructing spatial/temporal variations in BB through use of proxy records, such as charcoal in sediments and aerosol-borne chemicals in ice cores (Marlon et al., 2009, 2016; Power et al., 2008, 2012; Rubino et al., 2015). These records provide a qualitative assessment of past fires but do not constrain fire emissions on a global scale. Historical variations in BB trace gas emissions have been inferred from ice core records of methane, carbon monoxide (CO), and ethane (Bock et al., 2017; Ferretti et al., 2005; Mischler et al., 2009; Nicewonger et al., 2016; 2018; Sapart et al., 2012; Wang et al., 2010). The ice core records of these gases imply that major variations in BB have occurred over the past millennium, but interpretation of these records is complicated by the fact that each of these gases have major sources other than BB.

Acetylene is a nonmethane hydrocarbon released from incomplete combustion of biomass (including wildfires, land clearing, and agricultural waste), biofuels used for heating and cooking, and fossil fuels (Whitby & Altwicker, 1978; Xiao et al., 2007). Acetylene may also be released from partial combustion of methane during geologic outgassing, although this source is not well quantified (Anderson, 1958; Gunter & Musgrave, 1971; Liu et al., 2017). Global acetylene emissions today are estimated to be about 7 Tg y^{-1} , with roughly half attributed to biofuel combustion, and the remainder equally distributed between fossil fuel and BB emissions (Xiao et al., 2007). Acetylene is destroyed in the atmosphere via reaction with the hydroxyl radical

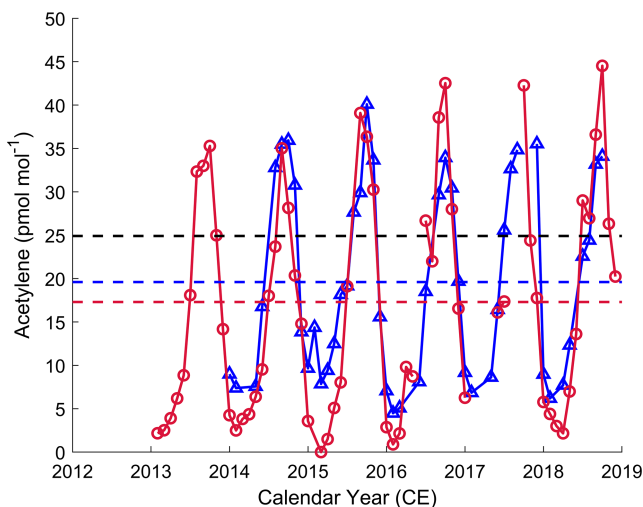


Figure 1. Atmospheric acetylene measurements from the high southern latitudes from 2013 to 2018 CE. NOAA-GMD surface air flasks from Cape Grim, Australia (blue triangles) and the South Pole (red circles) were measured at UC Irvine. Each data point represents the average of all samples in the same month. The annual mean at the Cape Grim and the South Pole sites are shown with the blue and red dashed lines, respectively. The estimated annual mean at the southern hemisphere high latitudes based on the Xiao et al. (2007) budget and our CTM-based source sensitivities is shown as the black dashed line.

under vacuum (Nicewonger, 2019; Nicewonger et al., 2016, 2018). The wet-extraction (melt) system consists of a glass extraction chamber and a glass vacuum line with Teflon-sealed glass isolation valves (Glass Expansion Australia) and flat glass flanges sealed with indium O-rings (Indium Wire Extrusion) connecting different sections. Samples are mechanically cleaned prior to analysis in a walk-in freezer using a scalpel blade, then placed in the glass extraction chamber precooled to $-40\text{ }^{\circ}\text{C}$. The sample chamber is connected to the vacuum line and repeatedly flushed with N_2 prior to extraction and it is isolated from the vacuum line while the sample melts. The released air is cryogenically dried and condensed into a stainless-steel tube immersed in liquid helium (4 K).

Acetylene is analyzed by gas chromatography (Agilent 6890 equipped with a DB-1 column) and high-resolution mass spectrometry (Waters AutoSpec Ultima) in EI+ mode at a nominal mass resolution of 8,000 ($m/\Delta m$). Acetylene is quantified using the parent ion at $m/z = 26.016$. An internal standard of ^{13}C -ethane is added to each sample to correct for instrument sensitivity changes (Aydin et al., 2007; Nicewonger et al., 2016, 2018). The ^{13}C -ethane peak is detected within the same mass function as acetylene roughly 10 s after the acetylene peak. Acetylene elutes between ethylene and ethane and is baseline-resolved (Figure S1). The calibration is based on standards prepared at UC Irvine (see SI Text S4 and Figure S2). All ice core data are solubility corrected (see SI Text S6).

Modern atmosphere acetylene measurements from the high southern latitudes are limited. We measured acetylene in glass flasks from the South Pole, Antarctica (2,810-m elevation) and Cape Grim, Australia (40.63°S , 94-m elevation) from the NOAA-GMD Halocarbons and other Atmospheric Trace Species group (<https://www.esrl.noaa.gov/gmd/hats/>). The bimonthly flask air samples were analyzed utilizing the same instrument and calibration as the ice core samples. There are two flasks from each sampling date and one of the flasks is analyzed twice, resulting in three measurements for each sampling date. Monthly averages of flask air acetylene are shown in Figure 1 (see supporting information for flask data quality control).

2.2. Chemistry Transport Modeling

Acetylene is short-lived and a three-dimensional chemistry transport modeling is used to estimate the response (or sensitivity) of acetylene over Greenland and Antarctica to emissions from various sources. Sensitivities depend on the spatial and seasonal distributions of the sources, atmospheric transport, and

(OH), with a global average lifetime of roughly 2–3 weeks (Xiao et al., 2007; Burkholder et al., 2015). Acetylene is not highly reactive with the Cl atom (Burkholder et al., 2015). Acetylene is considered a short-lived gas because the atmospheric lifetime is less than the typical tropospheric interhemispheric transport time (Law et al., 2007).

BB emissions are likely the only major source of acetylene in the atmosphere prior to the increase in fossil fuel and biofuel emissions in the industrial era. Due to the simplicity of the preindustrial acetylene budget, we propose that ice core acetylene measurements can be interpreted as a straightforward proxy for paleofire emissions. Here we (1) report the levels of atmospheric acetylene over the last 2,000 years measured in air extracted from Antarctic and Greenland ice cores, (2) compare these data to modern measurements of acetylene over Antarctica and Greenland and to other fire proxies from the last 1,000 years, and (3) utilize a chemistry transport model to estimate past acetylene BB emissions.

2. Methods

2.1. Ice Core and Surface Air Measurements

Acetylene was measured in the GISP2B ($n = 6$) and GISP2D ($n = 59$) ice cores from Summit, Greenland; the WDC05A ($n = 19$) and WDC06A ($n = 47$) ice cores from the West Antarctic Ice Sheet Divide, Antarctica; and the SPC14 ($n = 34$) ice core from the South Pole, Antarctica (see supporting information for ice core sites and chronologies). Ice core air bubbles were extracted from 300- to 380-g samples by melting the sample

photochemical reactivity, all of which are based on a modern-day atmospheric simulation with the University of California, Irvine-Chemistry Transport Model (UCI-CTM) run at $2.8^\circ \times 2.8^\circ$ horizontal resolution and 57 vertical layers (Holmes et al., 2013; Prather & Hsu, 2010). Tracer transport is driven by forecast seasonal meteorological fields from the European Center for Medium-Range Weather Forecasting. The tropospheric chemistry is described in Holmes et al. (2013). Fossil fuel emissions of acetylene are based on the Representative Concentration Pathway year 2000 inventories from Lamarque et al. (2010). BB emissions of dry matter are from the Global Fire Emissions Database version 3.1 (GFED3.1; van der Werf et al., 2010). Emission factors (g compound emitted/kg dry matter burned) are used to calculate BB emissions of acetylene from dry matter emissions (Akagi et al., 2011). The methane lifetime due to OH oxidation in the UCI-CTM is 8.9 years, which is 25% lower than the observation-based OH methane lifetime of 11.2 years (Prather et al., 2012). We scale the OH reaction rate coefficient for acetylene by a factor of 0.75 to produce an acetylene lifetime consistent with the observation-based methane lifetime (see supporting information for details). Simulations are conducted for a three-year period using meteorological fields from 2005 to 2007 and the final year (2007) is used to calculate annual-average surface acetylene mole fractions relative to dry air.

Tracer experiments are designed to estimate the sensitivity of acetylene levels over Greenland and Antarctica to small changes in emissions from various spatial/temporal geographic patterns of acetylene sources. This approach differs slightly from that used by Nicewonger et al. (2018). Here we model several acetylene-like species (same molecular weight and chemistry) emitted from different source regions (i.e., there are no background acetylene emissions from other sources). Each species is denoted by its source region, and each decays as acetylene, but the background chemistry and OH field are not affected.

In the simulations, acetylene mole fractions (pmol mol^{-1}) are calculated as the average over the air mass from surface up to about 500 hPa over $60\text{--}90^\circ\text{N}$ for Greenland and $60\text{--}90^\circ\text{S}$ for Antarctica. The sensitivity of acetylene is calculated in units of pmol mol^{-1} per Tg y^{-1} of acetylene emissions from a particular source. Sensitivities are computed for Greenland and Antarctica for acetylene emissions from BB, biofuels, fossil fuels, and geologic emissions (Table S1). Sensitivities are also calculated for BB emissions from different geographic regions (Tables S1 and S2). The model results show that Greenland and Antarctica exhibit similar sensitivities to nonboreal (90°S to 50°N) emissions and that Greenland is most sensitive to boreal ($50\text{--}90^\circ\text{N}$) emissions.

In all scenarios, biofuel emissions of acetylene are fixed at 0.5 Tg y^{-1} based on van Aardenne et al. (2001). Total atmospheric levels of acetylene are calculated for each scenario by combining various combinations of emission sources, scaled by the sensitivity of that source. The modeled Greenland and Antarctic acetylene levels are compared to the ice core observations (Table S3). Emission scenarios are evaluated for the two defined time periods by using the following functions:

$$\Delta_{\text{acetylene, grn}} = \frac{|m_{\text{grn}} - \bar{o}_{\text{grn}}|}{\bar{o}_{\text{grn}}} \quad (1)$$

$$\Delta_{\text{acetylene, ant}} = \frac{|m_{\text{ant}} - \bar{o}_{\text{ant}}|}{\bar{o}_{\text{ant}}} \quad (2)$$

where m is the modeled acetylene level and \bar{o} is the observed mean level of acetylene from the ice core record from Greenland (grn) and Antarctica (ant; Table S3). Emission scenarios are considered viable if $\Delta_{\text{acetylene, grn}}$ and $\Delta_{\text{acetylene, ant}}$ are <0.1 and rejected if $\Delta_{\text{acetylene, grn}}$ or $\Delta_{\text{acetylene, ant}}$ are >0.1 .

3. Results

3.1. Acetylene Surface Data

Atmospheric acetylene levels over Cape Grim, Australia and South Pole, Antarctica from 2013 to 2018 CE are similar, with annual averages in the range of $18\text{--}20 \text{ pmol mol}^{-1}$ (Figure 1). Acetylene levels across the high southern latitudes are relatively uniform, in agreement with global chemistry transport modeling (see Figure S3). The observed acetylene levels are in reasonable agreement with the Xiao et al. (2007) global acetylene budget. Using the UCI-CTM sensitivities described in section 2.2, the Xiao et al. (2007) budget yields

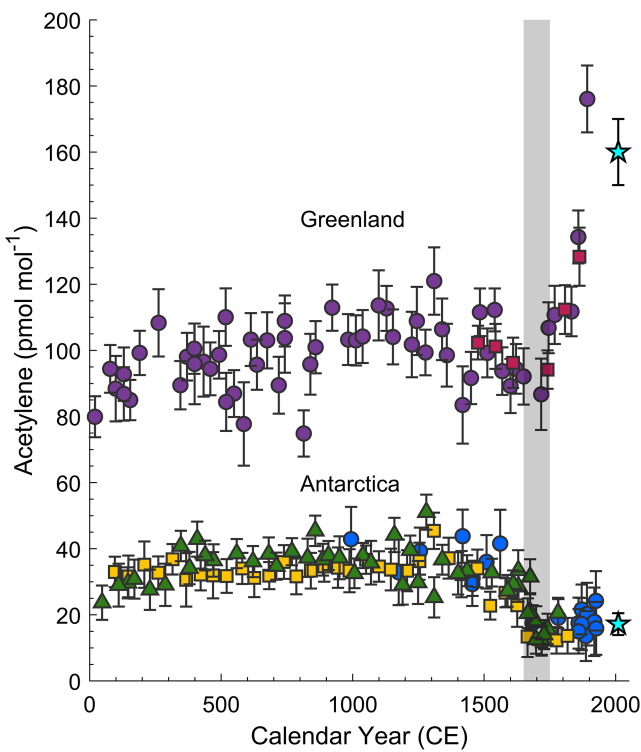


Figure 2. Ice core acetylene levels over the last 2,000 years. Greenland samples are from GISP2B (pink squares) and GISP2D (purple circles). Antarctic samples are from WDC05A (blue circles), WDC06A (green triangles), and SPC14 (yellow squares). Error bars represent $\pm 1\sigma$ analytical uncertainty (blanks and calibration) and a 15% solubility correction was applied to all data (Text S6). Mean acetylene levels over Greenland and Antarctica from 2012 to 2018 (cyan stars) are also shown. The gray bar delineates the acetylene minimum in both records from 1650 to 1750 CE that is used in the modeling work.

$17 \pm 2 \text{ pmol mol}^{-1}$ during 1650–1750 CE. For comparison, the annual mean acetylene over Antarctica today is $18\text{--}20 \text{ pmol mol}^{-1}$, about half of which is attributed to fossil-fuel and biofuel combustion (Xiao et al., 2007). Unlike Greenland, the Antarctic record does not display a sharp rise during the nineteenth or twentieth century.

4. Inferring BB Emission of Acetylene From Ice Core Records

The model-derived sensitivities are used to explore a wide range of emission scenarios that could reproduce the ice core acetylene data, assuming that acetylene variability was driven solely by changes in emissions. We assume constant acetylene lifetime based on model results that show preindustrial-to-modern atmospheric OH difference was in the range of +2 to -8% (Naik et al., 2013; Nicewonger et al., 2018). We also assume that atmospheric transport did not change. The emission scenarios cover the period from 1000 to 1750 CE. Acetylene variability prior to 1750 CE is assumed to be driven by BB only. Biofuel emissions are assumed to remain constant at 0.5 Tg y^{-1} (van Aardenne et al., 2001). The scenarios do not extend past 1750 CE because Northern Hemisphere acetylene levels increased sharply at that time, likely due to increasing anthropogenic emissions (Figure 2). Boreal ($>50^\circ\text{N}$) and nonboreal (90°S to 50°N) BB emissions must be allowed to vary independently in order to simulate both Antarctic and Greenland acetylene records (Figure 3).

During the Medieval Period (MP; 1000–1500 CE), 5.0 Tg y^{-1} of nonboreal and 0.6 Tg y^{-1} of boreal BB emissions are required to achieve agreement with the ice core records. Nonboreal BB emissions decline by about 55% from the MP to the Little Ice Age (LIA; 1650–1750 CE), while boreal emissions remain roughly constant.

acetylene levels over Antarctica of roughly 25 pmol mol^{-1} , slightly higher than the observations (Figure 1). These observations were made nearly a decade after the Xiao et al. (2007) budget was developed. Global acetylene emissions likely declined during that period (Worton et al., 2012).

Acetylene levels over Greenland are considerably greater than those over Antarctica, with a mean level of about $150 \pm 30 \text{ pmol mol}^{-1}$ during the 2013–2017 period (Helmig, 2017). The estimated acetylene level over the high northern latitude region based on the Xiao et al. (2007) global acetylene budget and the source sensitivities calculated from the UCI-CTM is roughly $205 \text{ pmol mol}^{-1}$. Similarly, Greenland acetylene abundance appears to have declined since the Xiao et al. (2007) budget. The large N/S asymmetry in acetylene results from the unequal hemispheric distribution of fossil fuel combustion and biofuel use combined with the atmospheric lifetime of acetylene being much shorter than the interhemispheric mixing time.

3.2. Acetylene Ice Core Records

The ice core acetylene records reveal significant temporal variability in atmospheric levels over the past 2,000 years (Figure 2). The Greenland ice core data show preindustrial acetylene levels that are considerably lower than the modern atmosphere throughout the 2,000-year record, indicating less acetylene emissions in the preindustrial Northern Hemisphere. The Greenland record displays a slow long-term increase during the first 1,000 years and later stabilizes, averaging $104 \pm 2 \text{ pmol mol}^{-1}$ (mean $\pm 1 \text{ SE}$) from 0 to 1500 CE. There is a clearly resolved minimum centered around 1700 CE, following a decline that starts near 1500 CE. Greenland levels rise sharply after 1750 CE.

The Antarctic acetylene data show a similar stability to Greenland over 0–1500 CE, with a sharp long-term decline that starts around 1500 CE. The Antarctic acetylene averages $36 \pm 1 \text{ pmol mol}^{-1}$ from 0 to 1500 CE, which is roughly twice the modern mean acetylene level over Antarctica. After 1650 CE, acetylene declines by more than 50% to a minimum of

These estimates are significantly greater than modern BB emissions based on the Global Fire Emissions Database Version 4, by a factor of 4 during the MP and by a factor of 2.5 during the LIA (van der Werf et al., 2017). This implies large changes to the global BB regime from preindustrial to modern, or a large underestimation of current BB emissions (Giglio et al., 2013; 2018). This analysis also implies a change in the spatial distribution (boreal vs. nonboreal) of the emissions between the MP and LIA, with boreal emissions accounting for 12% of total BB emissions during the MP and 26% during the LIA.

There are several caveats to these interpretations. For example, we do not consider changes to the geographic distribution of BB emissions. If the spatial distribution of BB emissions in the past was different than today, then the total BB emissions inferred from the ice core data would change. Antarctic acetylene is more sensitive to emissions from South America than from Africa or Australia (Table S1). If we assume that a much larger fraction of BB emissions during the MP occurred in South America, less emissions would be required to reconstruct the observed ice core levels. For the most extreme case, in which all nonboreal BB emissions were in South America, about 2.6 Tg y^{-1} of total BB emissions are required to reproduce the ice core acetylene data during the MP (Figure S4). Although this is less than half the total BB emissions needed during the MP for the base case (Figure 3), it is still twice the modern-day estimate of total acetylene emissions from BB. Thus, changes in the spatial distribution of burning is unlikely to alter the fundamental conclusion that BB during the MP was significantly greater than modern.

In the model scenarios, preindustrial biofuel emissions are assumed to have been lower than today and constant (0.5 Tg y^{-1}). Epidemics resulting from the arrival of Europeans in the new world reduced indigenous populations in the Americas by as much as 90% over the sixteenth century (Koch et al., 2019). This dramatic change in human population likely impacted both the magnitude and location of BB and biofuel emissions in South America. Higher biofuel emissions in the preindustrial period would reduce the BB emissions needed to match the ice core levels, both pre- and post-1500 CE (Figure S4 and Table S4). A model simulation was conducted to investigate the sensitivity of the inferred BB acetylene emission scenario to changes in the magnitude and location of the biofuel source. The inclusion of more biofuels in the model weighted toward the Northern Hemisphere (as is the case today) has little influence on Antarctic acetylene. The inclusion of a tropics-centered biofuel source is one-to-one interchangeable with BB emissions from the same region. Therefore, a tropical biofuel source would have no impact on the inference that global fire emissions (BB + biofuel) were higher during the MP than the modern atmosphere.

Acetylene budgets for the modern atmosphere do not include a geologic source because acetylene is not a significant component of natural petroleum hydrocarbons (Faramawy et al., 2016). Natural flaring of geologic emissions occurs when volcanic or hydrothermal activity causes ignition of hydrocarbon seeps and can lead to acetylene production from methane combustion (Dimitrov, 2002). If such sources were significant, it would reduce the BB and biofuel emissions required to reconstruct the observed ice core levels. Geologic emissions are located primarily in the Northern Hemisphere and influence Greenland acetylene more strongly than Antarctic acetylene (Table S1). Using the distribution of geologic sources from Etiope and Ciccioli (2009), we estimate that the maximum allowable geologic acetylene source is around 1.5 Tg y^{-1} (Figure S4 and Table S4). At this extreme case of geologic emissions, acetylene emitted from boreal fires essentially drops to zero. Under this scenario, 3.8 Tg y^{-1} of nonboreal BB emissions are necessary to match the ice core records from both hemispheres during the MP. For geologic emissions of less than 1.0 Tg y^{-1} acetylene, total BB emission of acetylene in the preindustrial period is larger in the MP and LIA than the modern day.

5. Comparing Acetylene to Other BB Proxies

For the past millennium, there are some similarities between various BB proxies and also some significant differences. Like acetylene, the other proxies show the LIA as a minimum in burning (Figure 3). From the MP to the LIA, a gradual decline in atmospheric $\delta^{13}\text{CH}_4$ suggests a 30–40% decline in BB emissions (Ferretti et al., 2005; Mischler et al., 2009). Ethane levels in Antarctic ice cores also decline by 30–45% during the same period (Nicewonger et al., 2018). CO also exhibits a minimum during the LIA, but this occurs following a steep decline from 1400 CE onward, which is not exhibited in the other trace gas records. Charcoal influx is consistent with the trace gas records; in that, it is relatively steady during the MP prior to the LIA decline. CO and charcoal influx are markedly different from the other trace gases; in that, they show a steep

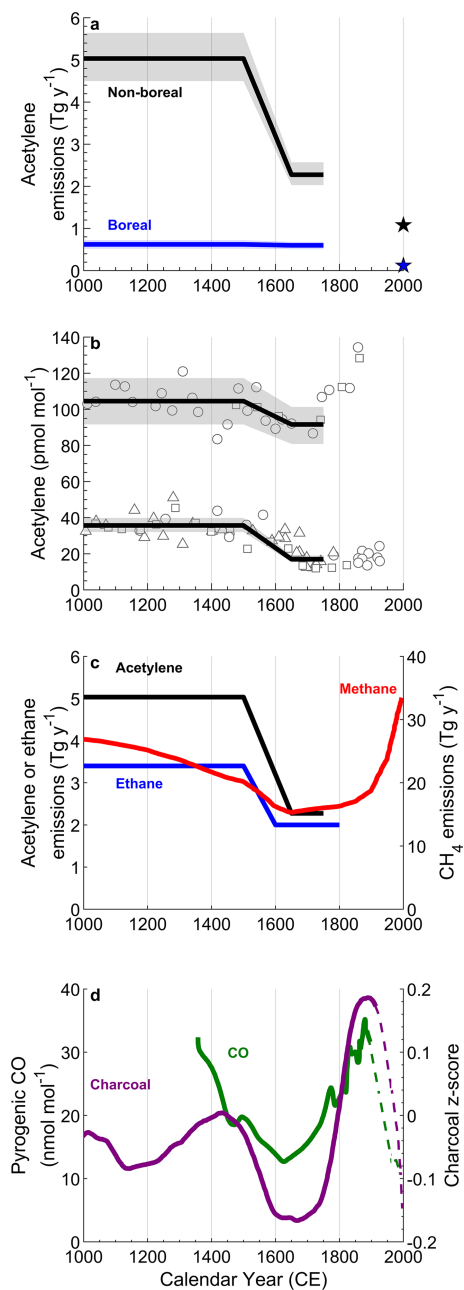


Figure 3. Inferred biomass burning acetylene emissions, the resulting mixing ratio over Greenland and Antarctica from these emissions, and a comparison of the inferred acetylene biomass burning emissions with other proxies for the last 1,000 years. (a) Boreal and nonboreal acetylene emissions: mean $\pm 1\sigma$ (solid lines and shaded band). The shaded band reflects uncertainty in emissions, emission factors, and the solubility correction (supporting information Text S6). Estimate of boreal and nonboreal biomass burning acetylene emissions in the modern atmosphere are shown for reference (black and blue stars; van der Werf et al., 2017). (b) Acetylene over Greenland (top) and Antarctica (bottom) resulting from the emission scenario in (a), using the same symbols as in Figure 2. (c) Nonboreal ethane emissions (blue; left axis; Nicewonger et al., 2018), nonboreal acetylene emissions (black; left axis; this study), and pyrogenic methane emissions (red; right axis; Ferretti et al., 2005). (d) Pyrogenic CO (green; left axis; Wang et al., 2010) and global charcoal influx (purple, right axis; Marlon et al., 2009). Uncertainties on emissions in (c) and (d) are excluded for simplicity.

rise beginning prior to 1750, culminating in a maximum in the late 1800s. By contrast, acetylene, ethane, and methane all indicate that burning remained low throughout the 1800s.

There are several factors that might contribute to the apparent difference in these BB proxies. For example, the preindustrial methane and ethane budgets are complicated by a larger variety of emission sources. The interpretation of the ice core $\delta^{13}\text{CH}_4$ data depends on assumptions on the temporal stability of the methane isotopic end-members as well as the magnitude of the geologic source. The changes in the BB source of ethane during this period also depend heavily on the assumed background geologic emissions. There is also additional complexity in both methane and ethane budgets on the removal side via Cl oxidation. Furthermore, interpreting BB emissions from the methane and CO ice core records requires knowledge about stable-isotope biogeochemistry of these gases, which includes complexities such as possible source isotope signature changes through time (Rubino et al., 2015; Schwietzke et al., 2016). Acetylene has a less complicated preindustrial budget and does not require comeasurements of stable isotopes to interpret a preindustrial budget, therefore making it a more straightforward tracer for paleo-BB emissions than other trace gases. The relatively short lifetime of acetylene introduces a challenge; in that, the ice core record is sensitive to both the magnitude and geographic location of burning. This also presents an opportunity to gain insight from interpolar differences and to integrate ice core data with more qualitative regional information about BB trends and biogeography.

6. Conclusions

The ice core acetylene records indicate changes in global BB emissions over the past two millennia that impacted atmospheric composition in both hemispheres. BB emissions of acetylene were substantially greater than today for an extended period during the late preindustrial period from 0 to 1500 CE. While the modern BB acetylene budget may be underestimated by at least 25% due to biases in satellite observations (Giglio et al., 2013; 2018), a revision of that magnitude does not alter our conclusion that BB sources of acetylene during the MP were higher than today. Model simulations support this finding even allowing for (1) significant relocation of BB emissions, (2) the inclusion of a larger and more tropically located biofuel source, and (3) the addition of a geologic acetylene source.

A subsequent decline in acetylene levels from around 1500 CE to a minimum around 1700 CE occurred at a time of when both climate and human population were changing rapidly (Koch et al., 2019; Mann et al., 2009). The ice core acetylene record does not provide attribution for the underlying cause of this decline in burning. It may have resulted from variability in natural climate-driven wildfires or human-induced fires linked to changes in human demography (land clearing, agricultural, or biofuel usage), or a combination of both (Ferretti et al., 2005; Power et al., 2012; Marlon et al., 2008; Neville & Bird, 2008; Dull et al., 2010; Pechony & Shindell, 2010; Koch et al., 2019).

There is qualitative agreement in the trends in BB emissions over the last 1,000 years inferred from ice core acetylene, ethane, and methane. Quantitatively, the decline in BB emissions between the MP and LIA inferred from the proxies is slightly larger for acetylene (50%) than for

methane and ethane (30–45%). There is no evidence in the three ice core hydrocarbon records for a large peak in fire emissions/activity in the late 1800s as suggested by the CO and charcoal records.

These first ice core acetylene measurements demonstrate the utility of this approach in reconstructing paleofire variability. An understanding of the relationship between climate and fire will be obtained by extending the acetylene records back in time to periods of smaller human influence and larger climatic change. Such records will help the development of dynamic fire models needed for projections of future fire in a warmer climate.

Acknowledgments

We thank Xin Zhu for the assistance with the UCI-CTM, Steve Montzka from NOAA GMD for sharing the surface flasks, and NSF-ICF and IDP for the ice core drilling and samples. This research was supported by NSF Grants OPP-1644245 and OPP-1142517, NSF GRFP Award DGE-1312846 (to M. R. N.), and NASA Grant NN1X15AE35G (to M. J. P.). The ice core and surface acetylene data are available online ([doi:10.18739/A2J09W45H](https://doi.org/10.18739/A2J09W45H) and <https://doi.org/10.7280/D1TD4D>).

References

- Akagi, S. K., Yokelson, R. J., Wiedinmyer, C., Alvarado, M. J., Reid, J. S., Karl, T., et al. (2011). Emission factors for open and domestic biomass burning for use in atmospheric models. *Atmospheric Chemistry and Physics*, 11(9), 4039–4072. <https://doi.org/10.5194/acp-11-4039-2011>
- Anderson, R. C. (1958). Acetylene as an intermediate in combustion of petroleum hydrocarbons. *Advances in Chemistry*, 20, 49–57. <https://doi.org/10.1021/ba-1958-0020.ch005>
- Aydin, M., Williams, M. B., & Saltzman, E. S. (2007). Feasibility of reconstructing paleoatmospheric records of selected alkanes, methyl halides, and sulfur gases from Greenland ice cores. *Journal of Geophysical Research*, 112(D7), D07312. <https://doi.org/10.1029/2006JD008027>
- Bock, M., Schmitt, J., Beck, J., Seth, B., Chappellaz, J., & Fischer, H. (2017). Glacial/interglacial wetland, biomass burning, and geologic methane emissions constrained by dual stable isotopic CH₄ ice core records. *Proceedings of the National Academy of Sciences*, 114(29), E5778–E5786. <https://doi.org/10.1073/pnas.1613883114>
- Bowman, D. M. J. S., Balch, J. K., Artaxo, P., Bond, W. J., Carlson, J. M., Cochrane, M. A., et al. (2009). Fire in the Earth system. *Science*, 324 (5926), 481–484. <https://doi.org/10.1126/science.1163886>
- Burkholder, J. B., Sander, S. P., Abbatt, J., Barker, J. R., Huie, R. E., Kolb, C. E., et al. (2015). *Chemical Kinetics and Photochemical Data for Use in Atmospheric Studies Evaluation No. 18*. Pasadena: JPL Publication 15-10, Jet Propulsion Laboratory. <https://jpldataeval.jpl.nasa.gov>
- Dimitrov, L. I. (2002). Mud volcanoes: The most important pathway for degassing deeply buried sediments. *Earth-Science Reviews*, 59(1–4), 49–76. [https://doi.org/10.1016/S0012-8252\(02\)00069-7](https://doi.org/10.1016/S0012-8252(02)00069-7)
- Dull, R. A., Nevel, R. J., Woods, W. I., Bird, D. K., Avnery, S., & Denevan, W. M. (2010). The Columbian Encounter and the Little Ice Age: Abrupt land use change, fire, and greenhouse forcing. *Annals of the Association of American Geographers*, 5608. <https://doi.org/10.1080/00045608.2010.502432>
- Etiope, G., & Ciccioli, P. (2009). Earth's degassing: A missing ethane and propane source. *Science*, 323(5913), 478. <https://doi.org/10.1126/science.1165904>
- Faramawy, S., Zaki, T., & Sahr, A. A. (2016). Natural gas origin, composition, and processing: A review. *Journal of Natural Gas Science and Engineering*, 34, 34–54. <https://doi.org/10.1016/j.jngse.2016.06.030>
- Ferretti, D. F., Miller, J. B., White, J. W. C., Etheridge, D. M., Lassey, K. R., Lowe, D. C., et al. (2005). Unexpected changes to the global methane budget over the past 2000 years. *Science*, 309(5741), 1714–1717. <https://doi.org/10.1126/science.1115193>
- Giglio, L., Boschetti, L., Roy, D. P., Humber, M. L., & Justice, C. O. (2018). The collection 6 MODIS burned area mapping algorithm and product. *Remote Sensing of Environment*, 217(July), 72–85. <https://doi.org/10.1016/j.rse.2018.08.005>
- Giglio, L., Randerson, J. T., & van der Werf, G. R. (2013). Analysis of daily, monthly, and annual burned area using the fourth-generation Global Fire Emissions Database (GFED4). *Journal of Geophysical Research – Biogeosciences*, 118, 317–328. <https://doi.org/10.1002/jgrc.20042>
- Gunter, B. D., & Musgrave, B. C. (1971). New evidence on the origin of methane in hydrothermal gases. *Geochimica et Cosmochimica Acta*, 35, 113–118. [https://doi.org/10.1016/0016-7037\(71\)90109-8](https://doi.org/10.1016/0016-7037(71)90109-8)
- Helmig, D. (2017). Atmospheric hydrocarbons as tracers for climate change, air transport, and oxidation chemistry in the Arctic, GEOSummit, Greenland 2008–2017. Arctic Data Center. <https://doi.org/10.18739/A2RSOX>
- Holmes, C. D., Prather, M. J., Sovde, O. A., & Myhre, G. (2013). Future methane, hydroxyl, and their uncertainties: Key climate and emission parameters for future predictions. *Atmospheric Chemistry and Physics*, 13(1), 285–302. <https://doi.org/10.5194/acp-13-285-2013>
- Koch, A., Brierley, C., Maslin, M. M., & Lewis, S. L. (2019). Earth system impacts of the European arrival and Great Dying in the Americas after 1492. *Quaternary Science Reviews*, 207, 13–36. <https://doi.org/10.1016/j.quascirev.2018.12.004>
- Lamarque, J. F., Bond, T. C., Eyring, V., Granier, C., Heil, A., Klimont, Z., et al. (2010). Historical (1850–2000) gridded anthropogenic and biomass burning emissions of reactive gases and aerosols: Methodology and application. *Atmospheric Chemistry and Physics*, 10(15), 7017–7039. <https://doi.org/10.5194/acp-10-7017-2010>
- Law, K. S., Sturges, W. T., Blake, D. R., Blake, N. J., Burkholder, J. B., Butler, J. H., et al. (2007). Chapter 2: Halogenated very short-lived substances. In *Scientific Assessment of Ozone Depletion: 2006*.
- Liu, Y., Zhang, Q., & Wang, T. (2017). Detailed chemistry modeling of partial combustion of natural gas for coproducing acetylene and syngas. *Combustion Science and Technology*, 189(5), 908–922. <https://doi.org/10.1080/00102202.2016.1256879>
- Mann, M. E., Zhang, Z., Rutherford, S., Bradley, R. S., Hughes, M. K., Shindell, D., et al. (2009). Global signatures and dynamical origins of the Little Ice Age and Medieval Climate Anomaly. *Science*, 326(5957), 1256–1260. <https://doi.org/10.1126/science.1177303>
- Marlon, J. R., Bartlein, P. J., Carcaillet, C., Gavin, D. G., Harrison, S. P., Higuera, P. E., et al. (2009). Climate and human influences on global biomass burning over the past two millennia. *Nature Geoscience*, 2(4), 307–307. <https://doi.org/10.1038/ngeo468>
- Marlon, J. R., Kelly, R., Daniau, A., Vannière, B., Power, M. J., Bartlein, P., et al. (2016). Reconstructions of biomass burning from sediment-charcoal records to improve data-model comparisons. *Biogeosciences (BG)*, 13(11), 3225–3244. <https://doi.org/10.5194/bg-13-3225-2016>
- Mischler, J. A., Sowers, T. A., Alley, R. B., Battle, M., McConnell, J. R., Mitchell, L., et al. (2009). Carbon and hydrogen isotopic composition of methane over the last 1000 years. *Global Biogeochemical Cycles*, 23(GB4024), GB4024. <https://doi.org/10.1029/2009GB003460>
- Naik, V., Voulgarakis, A., Fiore, A. M., Horowitz, L. W., Lamarque, J. F., Lin, M., et al. (2013). Preindustrial to present-day changes in tropospheric hydroxyl radical and methane lifetime from the Atmospheric Chemistry and Climate Model Intercomparison Project (ACCMIP). *Atmospheric Chemistry and Physics*, 13(10), 5277–5298. <https://doi.org/10.5194/acp-13-5277-2013>

- Nevle, R. J., & Bird, D. K. (2008). Effects of syn-pandemic fire reduction and reforestation in the tropical Americas on atmospheric CO₂ during European conquest. *Palaeogeography, Palaeoclimatology, Palaeoecology*, 264, 25–38. <https://doi.org/10.1016/j.palaeo.2008.03.008>
- Nicewonger, M. R. (2019). *Ice core records of ethane and acetylene for use as biomass burning proxies*. (Doctoral dissertation). Retrieved from <https://escholarship.org/uc/item/99z5r4hm> Location: University of California, Irvine.
- Nicewonger, M. R., Aydin, M., Prather, M. J., & Saltzman, E. S. (2018). Large changes in biomass burning over the last millennium inferred from paleoatmospheric ethane in polar ice cores. *Proceedings of the National Academy of Sciences*, 1–6. <https://doi.org/10.1073/pnas.1807172115>
- Nicewonger, M. R., Verhulst, K. R., Aydin, M., & Saltzman, E. S. (2016). Preindustrial atmospheric ethane levels inferred from polar ice cores: A constraint on the geologic sources of atmospheric ethane and methane. *Geophysical Research Letters*, 43, 1–8. <https://doi.org/10.1002/2015GL066854>
- Pechony, O., & Shindell, D. T. (2010). Driving forces of global wildfires over the past millennium and the forthcoming century. *Proceedings of the National Academy of Sciences*, 107(45), 19,167–19,170. <https://doi.org/10.1073/pnas.1003669107>
- Power, M. J., Marlon, J., Ortiz, N., Bartlein, P. J., Harrison, S. P., Mayle, F. E., et al. (2008). Changes in fire regimes since the last glacial maximum: An assessment based on a global synthesis and analysis of charcoal data. *Climate Dynamics*, 30(7–8), 887–907. <https://doi.org/10.1007/s00382-007-0334-x>
- Power, M. J., Mayle, F. E., Bartlein, P. J., Marlon, J. R., Anderson, R. S., Behling, H., et al. (2012). Climatic control of the biomass-burning decline in the Americas after AD 1500. *The Holocene*, 23(1), 3–13. <https://doi.org/10.1177/0959683612450196>
- Prather, M. J., Holmes, C. D., & Hsu, J. (2012). Reactive greenhouse gas scenarios: Systematic exploration of uncertainties and the role of atmospheric chemistry. *Geophysical Research Letters*, 39, 6–10. <https://doi.org/10.1029/2012GL051440>
- Prather, M. J., & Hsu, J. (2010). Coupling of nitrous oxide and methane by global atmospheric chemistry. *Science*, 330(6006), 952–955. <https://doi.org/10.1126/science.1196285>
- Rubino, M., D'Onofrio, A., Seki, O., & Bendle, J. A. (2015). Ice-core records of biomass burning. *The Anthropocene Review*, 3(2), 140–162. <https://doi.org/10.1177/2053019615605117>
- Sapart, C. J., Monteil, G., Prokopiou, M., van de Wal, R. S. W., Kaplan, J. O., Sperlich, P., et al. (2012). Natural and anthropogenic variations in methane sources during the past two millennia. *Nature*, 490(7418), 85–88. <https://doi.org/10.1038/nature11461>
- Schwietzke, S., Sherwood, O. A., Bruhwiler, L. M. P., Miller, J. B., Etiope, G., Dlugokencky, E. J., et al. (2016). Upward revision of global fossil fuel methane emissions based on isotope database. *Nature*, 538(7623), 88–91. <https://doi.org/10.1038/nature19797>
- van Aardenne, J. A., Dentener, F. J., Olivier, J. G. J., Klein Goldewijk, C. G. M., & Lelieveld, J. (2001). A 1 × 1 resolution data set of historical anthropogenic trace gas emissions for the period 1890–1990. *Global Biogeochemical Cycles*, 15(4), 909–928. <https://doi.org/10.1029/2000GB001265>
- van der Werf, G. R., Peters, W., van Leeuwen, T. T., & Giglio, L. (2013). What could have caused pre-industrial biomass burning emissions to exceed current rates? *Climate of the Past*, 9(1), 289–306. <https://doi.org/10.5194/cp-9-289-2013>
- van der Werf, G. R., Randerson, J. T., Giglio, L., Collatz, G. J., Mu, M., Kasibhatla, P. S., et al. (2010). Global fire emissions and the contribution of deforestation, savanna, forest, agricultural, and peat fires (1997–2009). *Atmospheric Chemistry and Physics*, 10(23), 11,707–11,735. <https://doi.org/10.5194/acp-10-11707-2010>
- van der Werf, G. R., Randerson, J. T., Giglio, L., van Leeuwen, T. T., Chen, Y., Rogers, B. M., et al. (2017). Global fire emissions estimates during 1997–2016. *Earth System Science Data*, 9(2), 697–720. <https://doi.org/10.5194/essd-9-697-2017>
- Wang, Z., Chappellaz, J., Park, K., & Mak, J. E. (2010). Large variations in southern hemisphere biomass burning during the last 650 years. *Science*, 330(6011), 1663–1666. <https://doi.org/10.1126/science.1197257>
- Whitby, R. A., & Altwickier, E. R. (1978). Acetylene in the atmosphere: Sources, representative ambient concentrations and ratios to other hydrocarbons. *Atmospheric Environment*, 12(6–7), 1289–1296. [https://doi.org/10.1016/0004-6981\(78\)90067-7](https://doi.org/10.1016/0004-6981(78)90067-7)
- Worton, D. R., Sturges, W. T., Reeves, C. E., Newland, M. J., Penkett, S. A., Atlas, E., et al. (2012). Evidence from firn air for recent decreases in non-methane hydrocarbons and a 20th century increase in nitrogen oxides in the Northern Hemisphere. *Atmospheric Environment*, 54, 592–602. <https://doi.org/10.1016/j.atmosev.2012.02.084>
- Xiao, Y., Jacob, D. J., & Turquety, S. (2007). Atmospheric acetylene and its relationship with CO as an indicator of air mass age. *Journal of Geophysical Research-Atmospheres*, 112, 1–14. <https://doi.org/10.1029/2006JD008268>

References From the Supporting Information

- Buizert, C., Cuffey, K. M., Severinghaus, J. P., Baggensos, D., Fudge, T. J., Steig, E. J., et al. (2015). The WAIS Divide deep ice core WD2014 chronology: Part 1—Methane synchronization (68–31 ka BP) and the gas age–ice age difference. *Climate of the Past*, 11(2), 153–173. <https://doi.org/10.5194/cp-11-153-2015>
- Casey, K. A., Fudge, T. J., Neumann, T. A., Steig, E. J., Cavitte, M. G. P., & Blankenship, D. D. (2014). The 1500 m South Pole ice core: Recovering a 40 ka environmental record. *Annals of Glaciology*, 55(68), 137–146. <https://doi.org/10.3189/2014AoG68A016>
- Cuffey, K. M., & Clow, G. D. (1997). Temperature, accumulation, and ice sheet elevation in central Greenland through the last deglacial transition. *Journal of Geophysical Research*, 102, 26,383–26,396. <https://doi.org/10.1029/96JC03981>
- Meese, D. A., Gow, A. J., Alley, R. B., Zielinski, G. A., Grootes, P. M., Ram, M., et al. (1997). The Greenland Ice Sheet Project 2 depth-age scale: Methods and results. *Journal of Geophysical Research*, 102, 26,411–26,423. <https://doi.org/10.1029/97JC00269>
- Mitchell, L. E., Brook, E. J., Sowers, T., McConnell, J. R., & Taylor, K. (2011). Multidecadal variability of atmospheric methane, 1000–1800 C.E. *Journal of Geophysical Research*, 116, G02007. <https://doi.org/10.1029/2010JG001441>
- Orsi, A. J., Cornuelle, B. D., & Severinghaus, J. P. (2012). Little Ice Age cold interval in West Antarctica: Evidence from borehole temperature at the West Antarctic Ice Sheet (WAIS) Divide. *Geophysical Research Letters*, 39, 1–7. <https://doi.org/10.1029/2012GL051260>
- Reid, R. C., Prausnitz, J. M., & Poling, B. E. (1987). *The properties of gases of liquids: Their estimation and correlation*, (4th ed.). New York: McGraw-Hill.
- Sander, R. (2015). Compilation of Henry's law constants (version 4.0) for water as solvent. *Atmospheric Chemistry and Physics*, 15, 4399–4981. <https://doi.org/10.5194/acp-15-4399-2015>
- Schwander, J., Sowers, T., Barnola, J.-M., Blunier, T., Fuchs, A., & Malaize, B. (1997). Age scale of the air in the summit ice: Implication for glacial-interglacial temperature change. *Journal of Geophysical Research*, 102, 19,483–19,493. <https://doi.org/10.1029/97JD01309>
- Sigl, M., Fudge, T. J., Winstrup, M., Cole-Dai, J., Ferris, D., McConnell, J. R., et al. (2016). The WAIS Divide deep ice core WD2014 chronology: Part 2—Annual-layer counting (0–31 ka BP). *Climate of the Past*, 12(3), 769–786. <https://doi.org/10.5194/cp-12-769-2016>

- Souney, J. M., Twickler, M. S., Hargreaves, G. M., Bencivengo, B. M., Kippenhan, M. J., Johnson, J. A., et al. (2014). Core handling and processing for the WAIS Divide ice-core project. *Annals of Glaciology*, 55(68), 15–26. <https://doi.org/10.3189/2014AoG68A008>
- Winski, D. A., Fudge, T. J., Ferris, D. G., Osterberg, E. C., Fegyveresi, J. M., ColeDai, J., et al. (2019). The SP19 chronology for the South Pole Ice Core: Part 1—Volcanic matching and annual layer counting. *Climate of the Past*, 15(5), 1793–1808. <https://doi.org/10.5194/cp-15-1793-2019>
- Yevich, R., & Logan, J. A. (2003). An assessment of biofuel use and burning of agricultural waste in the developing world. *Global Biogeochemical Cycles*, 17(4), 1095. <https://doi.org/10.1029/2002GB001952>